Title: Assessment of structure-activity relationships and biased agonism at the Mu opioid receptor of novel synthetic opioids using a novel, stable bio-assay platform

Authors: Vasudevan, L., Vandeputte, M., Deventer, M., Wouters, E., Cannaert, A., & Stove, C.

In: BIOCHEMICAL PHARMACOLOGY, 177, 2020

Optional: https://doi.org/10.1016/j.bcp.2020.113910

Assessment of structure-activity relationships and biased agonism at the Mu opioid receptor of novel synthetic opioids using a novel, stable bio-assay platform

Running title: Stable bio-assay platform to study Mu opioid receptor agonists

Lakshmi Vasudevan, Marthe Vandeputte, Marie Deventer, Elise Wouters, Annelies Cannaert, Christophe P. Stove*

Laboratory of Toxicology, Department of Bioanalysis, Faculty of Pharmaceutical Sciences, Ghent University, 9000 Ghent, Belgium

*Corresponding author: Christophe P. Stove,
Laboratory of Toxicology,
Department of Bioanalysis,
Faculty of Pharmaceutical Sciences,
Ghent University,
9000 Ghent, Belgium.
Tel.: +32 9 264 81 35.
E-mail: christophe.stove@ugent.be

The authors declare no conflict of interest

ORCID n°s:

Marthe Vandeputte: https://orcid.org/0000-0002-1431-441X

Marie Deventer: https://orcid.org/0000-0001-6667-2561

Elise Wouters: https://orcid.org/0000-0001-9117-4759

Annelies Cannaert: https://orcid.org/0000-0002-8654-1371

Christophe Stove: https://orcid.org/0000-0001-7126-348X

Abstract

Fentanyl and morphine are agonists of the Mu opioid receptor (MOR), which is a member of the GPCR family. Their analgesic effects are associated with unwanted side effects. On a signaling level downstream from MOR, it has been hypothesized that analgesia may be mediated through the G protein pathway, whereas the undesirable effects of opioids have been linked to the β-arrestin (βarr) pathway. Despite being an increasingly debated subject, little is known about a potential 'bias' (i.e. the preferential activation of one pathway over the other) of the novel synthetic opioids (NSO) -including fentanyl analogs- that have emerged on the illegal drug market. We have therefore developed and applied a novel, robust bio-assay platform to study the activity of 21 NSO, to evaluate to what extent these MOR agonists show biased agonism and to investigate the potential correlation with their structure. In addition, we evaluated the functional selectivity of TRV130, a purported G protein-biased agonist. We applied newly established stable bio-assays in HEK293T cells, based on the principle of functional complementation of a split nanoluciferase, to assess MOR activation via recruitment of a mini-Gi protein (GTPase domain of Gαi subunit) or βarr2. All but two of the tested NSO demonstrated a concentration-dependent response at MOR in both bio-assays. The developed bio-assays allow to gain insight into the βarr2 or G protein recruitment potential of NSO, which may eventually help to better understand why certain opioids are associated with higher toxicity. Adding to the recent discussion about the relevance of the biased agonism concept for opioids, we did not observe a significant bias for any of the evaluated compounds, including TRV130.

Keywords: New psychoactive substances; Mu opioid receptor; Mini-Gi; β-arrestin; Bio-assay

Abbreviations: AC, Adenylyl cyclase; APC, Allophycocyanin; Asp, Aspartate; AUC, Area under the curve; βarr, β-arrestin; BV, Brilliant violet; cAMP, Cyclic adenosine monophosphate; CB1, Cannabinoid receptor 1; CD8(TR), Truncated CD8; dNGFR, Truncated nerve growth factor receptor; EGFP, Enhanced green fluorescent protein; E_{max}, Maximal response provoked by a ligand; FDA, The Food and Drug administration; Gi, Inhibitory family of G proteins; GIRK, G protein-coupled inwardly-rectifying potassium channel; GPCR, G protein-coupled

receptor; GRK, G protein-coupled receptor kinase; GTP, Guanosine triphosphate; GTPγ[^{35}S], ^{35}S-labelled guanosine triphosphate; HEK293T, Human Embryonic kidney293T; His, Histidine; HM, Hydromorphone; LgBiT, Large BiT, large subunit of Nanoluciferase; mini-Gi, Engineered GTPase domain of the Gαi subunit; MOR, Mu opioid receptor; NanoBiT®, NanoLuc Binary Technology®; NDA, New drug application; NPS, New psychoactive substances; NSO, Novel synthetic opioids; pEC_{50}, Negative logarithm of EC_{50}; SAR, Structure-activity relationship; SD, Standard deviation; SEM, Standard error of the mean; SmBiT, Small BiT, small subunit of Nanoluciferase; TM, Transmembrane; Trp, Tryptophan.

1. Introduction

Fentanyl, its analogues and other opioids that belong to the emerging class of new psychoactive substances (NPS) are powerful analgesics that mediate their action primarily by binding to the Mu opioid receptor (MOR) [1,2]. Apart from their analgesic effects, these novel synthetic opioids (NSO) also elicit other effects such as euphoria and relaxation [3,4], making them attractive compounds on the illicit drug market [5,6]. Unfortunately, these opioids are also associated with undesirable side effects such as vomiting, constipation, hypotension and respiratory depression [7-9], the latter usually being responsible for death in overdose cases [10,11]. Therefore, one of the major goals in the field of opioid research is to develop drugs with improved analgesia but reduced side effects. In this context, considerable research efforts have been directed towards the development of biased ligands. Biased agonism is the ability of some ligands to bind and stabilize the receptor in alternative active conformations [12,13], thereby activating a specific signaling pathway over the other, hence aptly termed as "functional selectivity" [14]. Ligand bias has most extensively been studied for the 'conventional' signaling pathway via G proteins and for the βarr pathway [15]. A large interest in the clinical potential of biased signaling via MOR was triggered by findings suggesting that analgesia could be separated from the undesirable side effects of opioids [16]. A key driver for this was the study by Raehal and colleagues [17], reporting on the fact that βarr knockout mice did not suffer from the side effects of administered morphine, while retaining analgesia. This suggested the involvement of βarr-mediated pathways in the peripheral unwanted effects [17] and led to the proposition that a 'G protein-biased' ligand of MOR may prove to be therapeutically useful by selectively engaging only the G protein pathway, with little or no activation of the βarr pathway [18]. The quest for G protein-biased ligands led to the development of oliceridine (TRV130), having been referred to as the first systemically active ligand of MOR, and reported to be efficacious for G protein coupling, with little βarr recruitment to the receptor [19,20]. Although data from preclinical studies with oliceridine seemed promising, recent clinical studies failed to demonstrate a significantly broader therapeutic window in humans, when compared to the administration of morphine [21].

It is well-known that the structure and activity of a compound go hand-in-hand. Previously, structure-activity relationship (SAR) studies on fentanyls have highlighted the importance of stereochemistry on the analgesic activity of these compounds, e.g. *cis* isomers were found to be more potent than *trans* isomers for 3-alkyl analogues of fentanyl [22]. Modification of different groups in the core structure of fentanyl may have drastic effects on the binding to and activity at MOR. One such modification is the introduction of a carbomethoxy (e.g. in carfentanil) or methoxymethyl group at position 4 of the piperidine ring, resulting in increased binding and potency, while substitution of a 4-methyl group affected the potency to a lesser extent [22-25] (**Figure 1, Panel A**). However, only limited research has been done on variants with modifications at the propanamide moiety [26] (**Figure 1, Panel A**), which have newly emerged on the market during the past few years. Likewise, systematic studies on bias demonstrated by fentanyls are scarce [27,28] and for non-fentanyl designer opioids even non-existing, with a knowledge gap regarding a possible correlation of their structure with bias. In this regard, application of functional assays to study agonism at a very early level of receptor activation, i.e. coupling of G protein and recruitment of βarr2 to MOR, may aid in gaining a better insight into the potential influence of (a) certain group(s) on the observed function.

With this in mind, we have functionally evaluated a panel of 21 NSO, including 18 fentanyl analogues and 3 other emerging synthetic opioids. In addition, TRV130, a purported G protein-biased agonist, was added to the panel of studied compounds. This panel was primarily chosen based on the emergence of the compounds on the drug scene during the past years, also aiming at covering a structurally diverse set of analytes. These analytes were tested using two distinct, yet closely related MOR reporter bio-assays, evaluating the coupling of either mini-Gi [29,30] (representing G protein recruitment) or βarr2 to MOR. Stable HEK293T cell lines were established in which the NanoBiT® technology was applied, a tool developed to assess protein-protein interactions [31]. The principle is based on functional complementation of a split nanoluciferase, one part being fused to MOR, the other being fused to an intracellular protein that is recruited to the activated receptor. The βarr2 recruitment principle has previously been applied in our lab for the activity-based screening of biological samples for the presence of NSO, using transiently transfected cells [32]. In the current study, we have set up a

novel, stable MOR reporter system, based on the recruitment of a mini-Gi protein to activated MOR, along with a βarr2 recruitment assay (which was improved by making the expression of the reporter system stable). Both bio-assays were used to investigate the correlation between structural features of NSO with their activity. Moreover, having data available for the recruitment of two distinct proteins to the same receptor, evaluated in the same cellular background and with the same read-out, allowed us to assess biased agonism for this set of compounds.

2. Materials and Methods

2.1 Chemicals and reagents

The reference compounds acetylfentanyl **(1)**, fentanyl **(2)**, butyrylfentanyl hydrochloride **(3)**, 4-methoxybutyrylfentanyl hydrochloride **(4)**, 4-fluoroisobutyrylfentanyl hydrochloride **(5)**, valerylfentanyl hydrochloride **(6)** cyclopropylfentanyl **(7)**, cyclopentylfentanyl hydrochloride **(8)**, tetramethylcyclopropylfentanyl hydrochloride **(9)**, tetrahydrofuranylfentanyl **(10)**, acrylfentanyl hydrochloride **(11)**, crotonylfentanyl **(12)**, methoxyacetylfentanyl hydrochloride **(13)**, ocfentanil hydrochloride **(14)**, benzoylfentanyl **(15)**, phenylpropionylfentanyl **(16)**, furanylfentanyl hydrochloride **(17)**, alfentanil hydrochloride **(18)**, U-47700 hydrochloride **(19)**, U-49900 hydrochloride **(20)**, and AH-7921 **(21)**, were purchased from Chiron Pharmasynth AS (Trondheim, Norway). TRV130 **(22)** was purchased from AdooQ Bioscience (Irvine, CA, USA). Hydromorphone **(0)**, poly-D-lysine, fetal bovine serum (FBS), chloroquine and puromycin were purchased from Sigma-Aldrich (Steinheim, Germany). Anti- truncated nerve growth factor receptor (dNGFR) antibody coupled to allophycocyanin (APC) and anti-CD8 antibody coupled to brilliant violet (BV) were procured from Chromaprobe (Maryland Heights, MO, USA). Iscove's Modified Dulbecco's Medium (IMDM), a Calcium Phosphate Transfection kit, DMEM + GlutaMAX™, Opti-MEM® I Reduced Serum, trypsin-EDTA (0.05%), amphotericin B, penicillin and streptomycin were purchased from Thermo Fisher Scientific (Pittsburg, PA, USA). HEK293T cells (passage 20) were a kind gift provided by Prof. O. De Wever (Laboratory of Experimental Cancer Research, Department of Radiation Oncology and Experimental Cancer Research, Ghent University Hospital, Belgium). The Phoenix AMPHO packaging cell line was kindly provided by Prof. Bruno Verhasselt (Department of Clinical Chemistry, Microbiology, and Immunology, Ghent University, Belgium). The transfection reagent FuGENE® HD, Nano-Glo® Live Cell substrate furimazine and Nano-Glo® dilution buffer were procured from Promega (Madison, WI, USA). Methanol and acetonitrile were purchased from Biosolve Chemie (France).

2.2 Development of the transient MOR-NanoBiT®-mini-Gi reporter system

The optimal configuration of the MOR-NanoBiT®-mini-Gi reporter system for studying the coupling of mini-Gi to MOR was assessed by transient transfection of HEK293T cells with distinct combinations of MOR (MOR-LgBiT or MOR-SmBiT) and mini-Gi (mini-Gi-LgBiT, mini-Gi-SmBiT, LgBiT-mini-Gi and SmBiT-mini-Gi). Generation of the MOR and mini-Gi-fusion constructs has been described before [32,33]. On day one, HEK293T cells were seeded in a 6-well plate at a density of 5 x 10^5 cells/ well. On day two, the cells were transfected with different combinations of MOR and mini-Gi fusion constructs using FUGENE® HD reagent as per the manufacturer's protocol. On the third day, the cells were detached and re-seeded in a poly-D-lysine coated white 96-well plate at 5 x 10^4 cells/well, followed by overnight incubation. On the day of the experiment, the cells were washed with Opti-MEM® I Reduced Serum Medium to remove any interference from FBS and then 90 µL of this reduced serum medium was added. The substrate, furimazine, was prepared by diluting 20-fold with Nano-Glo® LCS dilution buffer and 25 µL was added to each well. Luminescence was monitored in a TriStar^2 LB 942 multimode plate reader which was controlled by ICE software (Berthold Technologies GmbH & Co., Bad Wildbad, Germany) until the signal stabilized (approximately 15 min). Next, 20 µl of (6.75x) concentrated MOR agonist hydromorphone (HM) **(0)** in Opti-MEM® I was added, to yield a final in-well concentration of 10 µM HM **(0)**. The choice for this concentration of HM stemmed from its previous use in a transient format of the MOR-βarr2 bio-assay, where 10 µM HM caused maximal receptor activation [32]. An appropriate blank (Opti-MEM® I) was also included and luminescence was measured for 120 min. The fold-light increase upon stimulation determined the optimal configuration of the MOR-mini-Gi system.

2.3 Development of the stable NanoBiT® reporter systems

The generation of the MOR-LgBiT and SmBiT-βarr2 constructs has been described previously [32,34]. For the generation of stable cell lines, constructs of interest had to be cloned in the retroviral vector system. The cloning of SmBiT-βarr2 and SmBiT-mini-Gi in the retroviral vector, pdLZRS-pBMN-link-I-dNGFR has been described elsewhere [33,35].

2.3.1 Cloning of MOR-LgBiT and GRK2 in retroviral vectors

The cloning of MOR-LgBiT and G protein-coupled receptor kinase 2 (GRK2; plasmid kindly provided by Laura Bohn [36]) in the retroviral vectors, respectively pdLZRS-IRES-EGFP and pdLZRS-IRES-CD8(TR)), was performed by Gateway® technology according to the manufacturer's protocol.

a. Construction of entry vectors containing the MOR-LgBiT and GRK2 coding sequences

First, MOR-LgBiT and GRK2 were PCR-amplified with their respective primers harbouring attB recombination sites (**Table 1**) using a Mastercycler™ Nexus Thermal Cycler (Eppendorf, Hamburg, Germany). Then, the amplified PCR product was sub-cloned into pDONR™, carrying attP sites. This reaction was catalyzed by BP Clonase™ enzyme mix (BP reaction) and subsequently the recombinant product was transformed in One Shot® Mach1™ T1 Phage-Resistant Chemically Competent *E. coli* (Thermo Fisher Scientific). The resultant recombinant products were the entry vectors of MOR-LgBiT and GRK2, flanked by attL sequences, in pDONR™. The kanamycin-resistant clones were checked by restriction digestion and confirmed by sequencing.

b. Construction of destination vectors containing the MOR-LgBiT and GRK2 coding sequences

In this step, the entry vectors of MOR-LgBiT and GRK2 in pDONR™, carrying attL recombination sites were cloned in their respective retroviral destination vectors, i.e. pdLZRS-IRES-EGFP and pdLZRS-IRES-CD8(TR), carrying attR sites. This reaction was catalyzed by LR Clonase™ enzyme mix (LR reaction) and recombinant products were used to transform One Shot® Mach1™ T1 Phage-Resistant Chemically Competent *E. coli*. Ampicillin-resistant clones were checked by restriction digestion and sequencing.

2.3.2 Development of stable MOR-NanoBiT® cell lines by retroviral transduction

a. Production of retrovirus using the PhoenixA packaging cell line

For the production of viruses, the Phoenix AMPHO (φNX-A) packaging cell line was used that was cultured at 37ºC, 7% CO_2 in IMDM supplemented with 10% heat-inactivated FBS, 2 mM glutamine, 100 IU/ml penicillin, 100 µg/ml streptomycin and 0.25 µg/ml amphotericin B (complete IMDM). These cells were transiently transfected with one of the retroviral expression vectors (carrying MOR-LgBiT, SmBiT-mini-Gi, SmBiT-βarr2 or GRK2) using the Calcium Phosphate tranfection kit, according to the manufacturer's protocol. The cells were kept under puromycin selection for 2 weeks and then the retroviral supernatant was harvested, spun for 10 min at 350 x g at 4ºC and aliquots of the supernatant were stored at -80ºC.

b. Development of a stable MOR-mini-Gi bio-assay

HEK293T cells were seeded in a 24-well plate at a density of 5 x 10^4 cells/well in complete DMEM. The next day, the medium was replaced by retroviral supernatant, consisting of a mixture of retroviruses containing MOR-LgBiT and SmBiT-mini-Gi (1:1), that was pre-incubated with 10 µL DOTAP Liposomal transfection reagent (Roche Diagnostics). The plates were centrifuged for 90 min at 950 x g at 32ºC in order to increase the transduction efficiency, which was assessed by flow cytometry after 48 h by checking the expression of enhanced green fluorescent protein (EGFP) (co-expressed with MOR-LgBiT) and dNGFR (co-expressed with SmBiT-mini-Gi). Assessment of the latter was done using an APC-linked antibody against NGFR.

c. Development of a stable MOR-βarr2-GRK2 bio-assay

All the steps were essentially the same as described above, except the retroviral transduction step. The retroviral transduction was performed in two steps. Initially, a mixture (1:1) of retroviruses containing MOR-LgBiT and SmBiT-βarr2 was used to transduce HEK293T cells. These cells were sorted for high expression of EGFP (MOR-LgBiT) and dNGFR (SmBiT-βarr2). Next, these sorted cells were

transduced using the GRK2 retroviral supernatant. The expression of GRK2 was assessed using an anti-CD8 antibody coupled to BV, as truncated CD8 (CD8(TR)) is co-expressed with GRK2.

d. Cell sorting of stably transduced HEK293T cells

The transduced HEK293T cells were sorted using a BD FACSAria III cell sorter (BD Biosciences). The cells were selected for high co-expression of the MOR-mini-Gi or MOR-βarr2-GRK2 by sorting based upon the co-expressed markers EGFP, dNGFR and CD8(TR). Post-sorting, the cells were cultured in complete DMEM with 10% FBS. The expression of MOR (via EGFP), mini-Gi and βarr2 (via dNGFR) and GRK2 (via CD8(TR)) was monitored regularly by flow cytometry.

2.4 Screening of synthetic opioids using stable MOR reporter assays

A panel of 21 synthetic opioids and TRV130 were tested using the two stable MOR reporter systems: MOR-mini-Gi bio-assay and MOR-βarr2-GRK2 (for simplicity further called MOR-βarr2) bio-assay. In the latter, SmBiT-βarr2 is recruited to MOR-LgBiT in the presence of GRK2, following receptor activation. Performance of the stable MOR reporter assays only implies a relatively short and straightforward protocol. First, cells are seeded on a poly-D-lysine coated, white 96-well plate at a density of 5 x 10^4 cells/well and incubated overnight in the incubator (37°C, 5% CO_2). The actual assay is performed the following day, as described in **section 2.2**. Concentrated (6.75x) ligand solutions prepared in Opti-MEM® were used and the luminescence was measured for 120 min. All stock solutions were provided in methanol, except for those of acrylfentanyl **(11)**, butyrylfentanyl **(3)** and furanylfentanyl **(17)**, which were in acetonitrile, and hence, 6.75x stock solutions were prepared in appropriate solvents. The final concentration of opioid in the well ranged from 10 pM - 10 µM (25 µM). A solvent control (blank) with 0.5-5% methanol or acetonitrile in Opti-MEM® I and a concentration gradient of the reference compound HM **(0)** was run in all experiments. HM was chosen as a reference agonist based on previous experience [37], to allow normalization between different plates and to allow comparison throughout different studies. All the steps in the assay, from the washing until the measurement, were performed at room temperature.

2.5 Data and statistical analysis

Curve fitting and statistical analyses for the experiments were performed using the GraphPad Prism software (San Diego, CA, USA). The absolute luminescence signals were first corrected for solvent control and inter-well variability. Concentration-responses (area under the curve; AUC) were normalized to the maximum response of the reference compound, HM **(0)**, that was arbitrarily set to 100%. A non-linear regression model with a Hill slope of 1 was fitted to the normalized responses, yielding the pharmacological parameters E_{max} (a measure of efficacy, relative to HM) and pEC_{50} (a measure of potency).

Using the pharmacological parameters obtained above, the pathway bias was calculated using the method described in [38,39]. The calculation of bias is a two-step procedure, where in the first step, Equation (1) is used to calculate $\Delta\log (E_{max}/EC_{50})$ for every compound, with HM **(0)** as the reference for both coupling of mini-Gi and βarr2.

$$\Delta log\ (E_{max}/EC_{50}) = log\ (E_{max}\ A/EC_{50}\ A) - log\ (E_{max}\ B/EC_{50}\ B) \quad \text{Equation (1)}$$

(where A: test compound and B: reference compound, which is HM **(0)** in this case)

In the second step, pathway bias is calculated for each compound according to equation (2):

$$\Delta\Delta log\ (E_{max}/EC_{50}) = \Delta log\ (E_{max}/EC_{50})_{\ pathway\ 1} - \Delta log\ (E_{max}/EC_{50})_{\ pathway\ 2} \quad \text{Equation (2)}$$

(where pathway 1 is mini-Gi coupling and pathway 2 is βarr2 recruitment)

The bias factor, corresponding to the mean $\Delta\Delta\log (E_{max}/EC_{50})$, was calculated from three independent experiments (each performed in duplicate) and was plotted together with the standard error of the mean (SEM) for each compound. Statistical analysis was carried out by non-parametric one-way ANOVA (Kruskal-Wallis), followed by post hoc Dunn's multiple comparison test, to test for significant differences between the reference (HM) **(0)** and the compounds.

For the selection of the optimal combination of mini-Gi coupling to the activated receptor, the results are expressed as mean fold change ± standard deviation (SD), with six replicates and statistical analysis by two-tailed t-test.

3. Results

3.1 Development of a stable MOR reporter assay for real-time assessment of coupling of mini-Gi

Mini-G proteins are engineered GTPase domains of Gα subunits that are capable of coupling to the GPCR upon stimulation with an agonist, much like the native heterotrimeric G protein [29,30]. Their small size, stability and the fact that they can couple to the receptor independent from Gβγ subunits, makes them ideal candidates for studying the G protein pathway [30]. As MOR is a Gi-coupled receptor, we developed a system based on NanoBiT® using mini-Gi protein. To select the optimal configuration, different combinations of mini-Gi and MOR tagged with the split fragments of nanoluciferase (SmBiT or LgBiT) were tested in transiently transfected HEK293T cells. Owing to ease in maintenance, high transfection efficiency and rapid growth kinetics observed for these cells, this cell line was chosen for this study. MOR, being a plasma membrane protein, was tagged with LgBiT or SmBiT at its C-terminus, while mini-Gi, being a cytosolic protein, was tagged with LgBiT or SmBiT either N- or C-terminally. This resulted in four set-ups that could be tested to find the optimal combination to be used for further study (**Figure 2**). Upon stimulation with 10 µM HM **(0)**, the largest fold increase, when compared to solvent control, was obtained for the combination in which the C-terminus of MOR was tagged with LgBiT and SmBiT was tagged N-terminally of mini-Gi. Hence, MOR-LgBiT/SmBiT-mini-Gi was chosen as the ideal set-up for further experiments.

A stable HEK293T cell line co-expressing MOR-LgBiT and SmBiT-mini-Gi was generated by retroviral transduction and cell sorting, to reduce the variability between assays owing to differences in transfection efficiencies, with an added advantage of simplifying and shortening the assay protocol

(omission of transfection step). The expression of both fusion proteins was monitored by means of the co-expressed markers via flow cytometry (**Figure 3**).

3.2 Stable MOR reporter assay for real-time assessment of recruitment of βarr2

We previously reported on the development of a MOR reporter assay based upon the recruitment of SmBiT-βarr2 to activated MOR-LgBiT, using transiently transfected cells [32]. In contrast to the mini-Gi bio-assay, the βarr2 recruitment bio-assay involves a third component, GRK2, which is known to enhance the morphine-induced recruitment of βarr2 to MOR [36]. We previously demonstrated that the presence of GRK2 is beneficial for the assay's sensitivity [32]. Keeping this information in mind, we set-up a stable reporter system in HEK293T cells by triple retroviral transduction with viruses for i) MOR-LgBiT, ii) SmBiT-βarr2 and iii) GRK2. The protein expression levels were monitored with the help of co-expressed markers by flow cytometry (**Figure 3**).

3.3 Evaluation of fentanyl and non-fentanyl analogues using the βarr2 and mini-Gi platforms

Importantly, the reporter systems we developed contained the same receptor configuration: MOR-LgBiT, which could either couple with SmBiT-mini-Gi or with SmBiT-βarr2. This is a highly relevant aspect of this study, as it is well-known that the set-up of a system may strongly determine the outcome, which becomes even more important when aiming at comparing the results of two set-ups. The reporter systems used here are maximally similar, as they make use of the same cellular context (HEK293T cells), the same MOR-LgBiT receptor construct (expressed at similar levels in both developed stable cell lines) and the same read-out (bioluminescence). The only difference between the two bio-assays lies in the nature of the recruited signal transduction molecule (SmBiT-mini-Gi *vs.* SmBiT-βarr2).

A panel of 21 NSO, including 18 fentanyl analogues and 3 emerging non-fentanyl synthetic opioids, and TRV130 were evaluated using both MOR reporter assays. A sigmoidal dose-response curve was obtained for all compounds, except for benzoylfentanyl **(15)**, and tetramethylcyclopropyl-fentanyl **(9)**,

for which no significant activity was observed (**Figure 4**). For all the compounds, **Table 2** lists both the efficacies (E_{max}, relative to HM, for which the E_{max} was arbitrarily set at 100%) and the potencies (pEC_{50}), as assessed by both bio-assays, while **Figure 5** shows a graphical comparison. Based on these pharmacological parameters, we also evaluated the bias of all evaluated compounds as described in [38,39] and performed statistical analysis. We did not observe a significant bias for the evaluated compounds when compared to the reference, HM **(0)** (**Figure 6**).

4. Discussion

Analgesia is primarily mediated by binding of both endogenous opiate peptides and exogenous opioids, encompassing natural (e.g. morphine), semi-synthetic (hydromorphone, hydrocodone, etc.) and synthetic (fentanyl and non-fentanyl analogues) compounds, to MOR [1,40]. This binding leads to the coupling with Gαi, subsequently leading to the inhibition of cAMP production [41,42], whereas the dissociated βγ subunits inhibit the L-type Ca^{+2} channels [41] and activate G protein-coupled inwardly-rectifying K^+ (GIRK) channels, with a subsequent efflux of K^+ ions [43,44]. This ultimately results in neuronal hyperpolarisation and reduced neuronal excitability [45]. Another major transducer, βarr, has a role in decoupling the receptor from the G proteins, ultimately culminating in internalization of the receptor [46,47]. In addition, these arrestins also serve as docking sites for other moieties, switching on G protein-independent intracellular signaling [47].

Undoubtedly, opioids, and fentanyls in particular, are powerful analgesics, with the latter being known for their low cardiovascular toxicity, rapid onset and short duration of action [22]. Recently, the number of fentanyl analogues and other designer opioids has rapidly increased, primarily via the introduction of modifications to existing structures, to produce novel, potent analogues. There are four key structural features that can be modified in the core structure of fentanyl, giving rise to different fentanyl analogues: a) the piperidine ring, b) the anilino phenyl ring, c) the phenethyl group, and d) the carboxamide moiety linked to the anilino-nitrogen (**Figure 1, Panel A**). SAR studies have shown that fentanyls with substitutions at the tertiary piperidinyl-nitrogen phenethyl moiety fit better into the hydrophobic cavity of the receptor [26]. Such studies are useful to gain insight about how ligand

features modulate ligand binding and to get a probable clue about ligand interactions with the receptor. The fentanyls used in this study were primarily classified based on the R_1 group (aliphatic, ether and aromatic) substitutions linked to the carboxamide in the core structure of fentanyl (**Figure 1**). We also included the structurally divergent alfentanil **(18)**, as well as 3 non-fentanyl NSO, U-47700 **(19)**, U-49900 **(20)** and AH-7921 **(21)**. For purposes of completeness with regards to the bias evaluation, also TRV130 **(22)**, a purported G protein-biased ligand, was included.

4.1 Efficacy (E_{max}) and Potency (pEC_{50}) values

When looking at the efficacies (**Figure 5A, Table 2**) of the compounds in both assays, it can be noticed that the majority of the compounds had a (somewhat) higher efficacy for mini-Gi coupling as compared to βarr2 recruitment. Valerylfentanyl **(6)**, 4-methoxybutyrylfentanyl **(4)**, U-47700 **(19)** and U-49900 **(20)** did not follow this general trend. Also, efficacies varied to a broader extent for mini-Gi coupling, whereas they appeared to be more clustered for the recruitment of βarr2. Interestingly, this observation is distinct from the pattern observed for mini-Gi and βarr2 coupling to the cannabinoid receptor 1 (CB1), in which a wide range of efficacies was observed for βarr2 [33]. This demonstrates that the spread in efficacies truly depends on the receptor under study and is not an intrinsic characteristic of the set-up. Most compounds were more efficacious than the reference HM **(0)** in both assays. Valerylfentanyl **(6)**, crotonylfentanyl **(12)**, 4-methoxybutyrylfentanyl **(4)**, furanylfentanyl **(17)** and TRV130 **(22)** acted as partial agonists relative to HM **(0)**, with E_{max} values ranging from approximately 25-85% for both mini-Gi coupling and recruitment of βarr2. An exception to this was U-49900 **(20)**, which behaved as partial agonist for mini-Gi coupling but as full agonist for βarr2 recruitment (though a plateau was not reached). Combining these data with a closer look at the structure of fentanyls with open-chain aliphatic R_1-groups suggests an influence of chain length on their efficacy (**Figure 1, Panel B** and **Figure 5A**). Shorter chain fentanyls such as acetylfentanyl **(1)** were more efficacious than butyrylfentanyl **(3)**, which in turn was more efficacious than valerylfentanyl **(6)**. Also, 4-methoxybutyrylfentanyl **(4)**, which carries a methoxy group on the anilino phenyl ring in addition to the aliphatic R-group on the carboxamide moiety, turned out to be a partial

agonist. Similarly, the addition of a methyl group to acrylfentanyl **(11)** led to the formation of crotonylfentanyl **(12)**, which behaved as a partial agonist compared to the former. On the other hand, acetylfentanyl **(1)**, the fentanyl analogue with the shortest R_1-group, was not found to be more efficacious than fentanyl **(2)**, which suggests that there are additional factors in addition to chain length that determine the efficacy.

The most efficacious ligands were alfentanil **(18)** and U-47700 **(19)**, which were 3- and 2-fold more efficacious than HM **(0)** for coupling of mini-Gi and βarr2, respectively. Next in line were some ligands that were clearly more efficacious than the reference HM **(0)** to induce coupling of mini-Gi, such as fentanyl **(2)**, acrylfentanyl **(11)**, cyclopropylfentanyl **(7)** (>2.5 fold) and 4-fluoroisobutyrylfentanyl **(5)**, U-47700 **(19)** and ocfentanil **(14)** (>2-fold). Interestingly, ocfentanil **(14),** which contains a fluorine atom at the *ortho* position on the anilino phenyl ring, was found to be slightly more efficacious in both bio-assays than methoxyacetylfentanyl **(13)**, which does not possess this substitution. When comparing 4-methoxybutyrylfentanyl **(4)** with butyrylfentanyl **(3)**, the latter was almost 1.5-2.5-fold more efficacious in both bio-assays, pointing at a negative effect of the 4-methoxy group.

An initial comparison of the potencies (**Figure 5B**, **Table 2**) indicated that the potencies of the compounds roughly clustered in a similar range for both pathways. The order amongst the potent fentanyls for the recruitment of βarr2 was cyclopropylfentanyl **(7)** > acrylfentanyl **(11)** = fentanyl **(2)** > ocfentanil **(14)** > furanylfentanyl **(17)** > crotonylfentanyl **(12)**, while furanylfentanyl **(17)** was found to be the most potent one when considering coupling of mini-Gi. The presence of the fluorine atom at the *ortho* position of the anilino phenyl ring in ocfentanil **(14)** made it 5 to 8 times more potent than methoxyacetylfentanyl **(13)** (devoid of this fluorine atom substitution) at coupling of mini-Gi and βarr2. The pEC_{50} of fentanyl for the mini-Gi assay (-7.16) is in line with that reported by McPherson *et al*. [48], wherein the potency of fentanyl was tested by a GTPγ[^{35}S] assay (-7.24). As was the case with the efficacy, also the potency of 4-methoxybutyrylfentanyl **(4)** was lower (approximately 2.5-fold) than that of butyrylfentanyl **(3)** in both bio-assays, again indicating a negative impact of the

methoxy group. Benzoylfentanyl **(15)** and tetramethylcyclopropylfentanyl **(9)** showed no coupling of mini-Gi or βarr2 to MOR. The least potent amongst the other 19 NSO, in both bio-assays, was U-49900 **(20)**, followed by alfentanil **(18)** and acetylfentanyl **(1)**, although the latter two were found to be more efficacious than HM **(0)** in both bio-assays. The relatively poor potency of alfentanil in our βarr2 recruitment assay (pEC_{50} of -6.16) is essentially the same as that obtained by McPherson *et al.* (pEC_{50} of -6.19), who also used an enzyme-fragment complementation assay to study βarr2 recruitment to activated MOR. Valerylfentanyl **(6)** showed a rather low potency for the recruitment of βarr2 although it was found to be slightly more potent for the coupling of mini-Gi to MOR. Other opioids, such as butyrylfentanyl **(3)**, cyclopentylfentanyl **(8)**, amongst others and TRV130 **(22)**, were equipotent when considering both pathways.

For the fentanyls with a closed chain alkane substitution (**Figure 1, Panel B**), we noticed a unique trend: the potency and efficacy in both signaling pathways decreased drastically with increasing ring size, from cyclopropylfentanyl **(7)** (C3) to cyclopentylfentanyl **(8)** (C5). The bulky nature of the ring structure in tetramethylcyclopropylfentanyl **(9)** may also be the reason for its diminished activity. Similarly, furanylfentanyl **(17)**, the compound with the smallest unsaturated aromatic R_1 group substitution (**Figure 1, Panel C**) proved to be the most potent amongst other members of this group. At the other side of the activity spectrum, benzoylfentanyl **(15)** showed no coupling of mini-Gi and βarr2 to MOR. We hypothesize that this could be attributed to steric hindrance introduced by the ring structure, which may in some way affect the binding of the ligand to the binding pocket of MOR or disrupt or modulate the ligand-receptor interactions, thus affecting the active conformation of the receptor. Further (docking and/or binding) studies are needed to address these postulations. The insertion of a flexible linker between the phenyl ring and the carboxamide moiety of fentanyl, as in phenylpropionylfentanyl **(16)**, may result in a less rigid structure, explaining the improved potency and efficacy of this compound compared to benzoylfentanyl **(15)**.

Steric hindrance may also explain the profound difference in activity of the non-fentanyl analogues (**Figure 1, Panel E**) U-47700 **(19)** and U-49900 **(20)**, the latter having ethyl instead of methyl groups

linked to the nitrogen atom attached to the cyclohexyl moiety. Although both acted as full agonists (relative to HM **(0)**) for the recruitment of βarr2, U-47700 **(19)** behaved as a full agonist in the mini-Gi coupling assay, as opposed to U-49900 **(20)**, which acted as a partial agonist. However, U-49900 **(20)** was ten-fold and close to thirty-fold less potent than U-47700 **(19)** in mini-Gi and βarr2 coupling, respectively. Also, another structural analogue of U-47700 **(19)**, AH-7921 **(21)**, displayed a reduced (1.5-2-fold) potency. Incorrect spacing of the different groups, rather than steric hindrance, may be the prime factor for this compound.

Docking studies found that fentanyl positions vertically into the binding pocket of MOR, which is the best fitting model [23]. Studies using site-directed mutagenesis have implied that Aspartate (Asp) 147 of TM3 of MOR acts as a counterion for the protonated nitrogen that is present in morphine as well in fentanyl. The interaction between this Asp residue and the *N*-phenethyl group (containing the protonated nitrogen) orients the molecule in such a way that the phenyl group is close to Histidine (His) 297 of TM6, where it may undergo a strong donor-acceptor interaction with the His imidazole ring. These two interactions have been proposed to be important for MOR activation by fentanyl and its analogues. In addition, the *N*-phenylpropanamide group has been proposed to be in close proximity to Tryptophan (Trp) 318, where the ethyl group of fentanyl may undergo non-polar interactions with the aromatic part of Trp 318, while the phenyl group is oriented towards His 319 of TM7 [23]. Application of this knowledge to our study adds in the possibility of Π-Π interaction between fentanyls possessing an aromatic R_1 group and His or Trp in the vicinity of this R_1 group, which might explain the potency of furanylfentanyl **(17)**. In contrast, as already mentioned, steric hindrance may pose a problem for other compounds.

4.2 <u>Pathway bias</u>

The concept of signaling bias has gained significant interest over the past few years and has been studied for multiple GPCRs such as the angiotensin II receptor 1, the D_2 dopamine receptor, the β-adrenergic receptors and MOR [49]. For MOR, several attempts have been made to develop biased ligands that stimulate the G protein pathway, with limited βarr pathway stimulation, given the claimed

association of the former with analgesia and of the latter with adverse effects [17,19,50,51]. However, following the underwhelming results of TRV130 in clinical trials, this concept is now increasingly being questioned [52,53].

It is well-recognized that making statements about bias is highly context-dependent [28,53,54]. When calculating bias, it is of utmost importance to identify if the bias is truly stemming from differences in agonism pattern employed by the ligand (true bias) or caused by the systems themselves, also known as 'apparent' bias due to inherent differences in the assays used for the pathways being studied [54]. For example, Schmid *et al.* reported that, relative to DAMGO, fentanyl favored βarr2 recruitment to MOR when studied by an enzyme-fragment complementation βarr2 assay and when compared to GTPγS binding assay. On the other hand, fentanyl behaved as a G protein-biased agonist when the GTPγS binding assay was replaced by an inhibition of cAMP accumulation assay. These apparently contradictory findings illustrate that the direction of bias may be dependent on the assay used to study biased agonism. Gundry *et al.* and Rajagopal *et al.* [38,49,56] have addressed the key points that need to be considered when making conclusions about ligand bias, some of which are i) the chosen assays for studying different signaling pathways should have similar levels of amplification, and ii) time-dependent data should be collected to avoid confounding results due to potential kinetic effects. A similar point was put-forth in the study by Klein Herenbrink *et al.* [57], in which it was shown that the time point at which the measurements are made, as well as the pathway(s) used for the read-out(s), may influence the apparent bias. Keeping this in mind, the highly similar nature of the bio-assays used in this study allowed us to gain insight into possible biased agonism, while minimizing the methodological differences between the two bio-assays. In line with the above-mentioned studies by Gundry *et al.* [38], Rajagopal *et al*. [49,56], and Herenbrink *et al*. [57], our set-up was based on recruitment of either mini-Gi or βarr2 to the receptor, an event proximal to the receptor. Moreover, we applied the same principle (bioluminescence) as a read-out, thus avoiding issues related to differences in signal amplification that may complicate the interpretation of the presence of bias. Furthermore, in

both bio-assays, the same receptor construct is used (MOR-LgBiT), expressed at similar levels in the same cellular background (HEK293T). **Figure 6** quantitatively illustrates bias. In this plot, compounds with values above zero are considered to show preferential coupling to mini-Gi, whereas those with values below zero show a preference for βarr2 recruitment. As a reference ligand (a compound that fully activates the system and defines the full potential of what could be measured in the assay) [28], we chose HM **(0)** (i.e. a ligand for which we assume it is non-biased). We did not observe a significant preference towards coupling of mini-Gi or recruitment of βarr2 to MOR for any of the tested NSO. Overall, the differences were quite limited (all bias scores lying within the range -0.27 to 0.26; implying less than 2-fold difference), certainly when compared to a similar set-up which was applied to assess biased agonism of synthetic cannabinoid receptor agonists, where bias scores were much more deviating from zero (-1.018 to 1.204) [33]. Interestingly, also the purported G protein-biased compound oliceridine (TRV130 **(22)**), was not significantly biased in our hands. Worth noting in this context is that also others *did* observe recruitment of βarr2 following MOR activation with TRV130 [51,58]. We cannot exclude that the purported bias, as observed in those studies, may be an "apparent bias", as we are the first to apply very similar set-ups to assess biased agonism of this ligand (cfr. supra). As we know that, for a similar set-up (but with CB1 instead of MOR, as well as for the 5-HT2AR (unpublished findings)) it *is* possible to find biased compounds, we consider it unlikely that the fact that we do not find significantly biased compounds is related to the applied methodology *per se* [33].

The (effect of) biased agonism at MOR is highly debated, if not controversial. Kliewer, Gillis and Hill *et al.*, conducting independent experiments in three different laboratories, very recently demonstrated the persistence of opioid-induced respiratory depression in βarr2 knockout mice, questioning the entire concept of seeking G protein-biased agonists in the quest for safer opioid analgesics [53]. At the ligand level, our study further adds to this discussion: besides the absence of significant biased agonism of any of the 21 evaluated NSO, also

TRV130, previously claimed to be biased, did not show biased agonism (in terms of recruitment of βarr2 or mini-Gi) in two systems that were maximally similar in set-up.

In summary, in this study, we developed two stable, highly similar, yet distinct bio-assays, based on recruitment of mini-Gi or βarr2 to MOR when activated by a panel of 21 NSO and a purported G protein-biased agonist, TRV130. Insights into SAR were gained for the NSO, the highly similar nature of the deployed bio-assays also allowing the assessment of biased agonism. Although we did not observe significant bias, this study adds valuable information to the increasingly discussed concept of biased agonism at MOR.

Acknowledgements

The Ghent University-Bijzonder Onderzoeksfonds (BOF) is acknowledged for the PhD fellowship of L. Vasudevan (BOF.DCV.20—BOF15/DOS/021) and for funding of A. Cannaert (BOF; PDO026-18) and C. Stove (BOF; 01N00814 and 01J15517). The Research Foundation Flanders (FWO) is also acknowledged for the PhD fellowship of M. Vandeputte (3S038719), the postdoc fellowship of A. Cannaert (12Y9520N) and project grant n° G069419N. E. Wouters was supported by a BRAIN project grant from the Belgian Science Policy (Belspo) Office. The authors declare no conflict of interest.

Author contributions

L.V. and C.S. designed the experiments. L.V., M.D. and M.V. performed the experiments. L.V. and M.V. analyzed and prepared the manuscript. E.W. and A.C. contributed to the generation of stable cell lines and C.S. provided guidance, supervised the project, reviewed and edited the manuscript.

Declaration of interest

None

Submission declaration and verification

The manuscript or portions of it has never been published by another journal or electronic publication and that it has not been submitted simultaneously for publication elsewhere.

References

1 Comer SD, Cahill CM. Fentanyl: Receptor pharmacology, abuse potential, and implications for treatment. Neurosci Biobehav Rev. 2018.

2 Solimini R, Pichini S, Pacifici R, Busardò FP, Giorgetti R. Pharmacotoxicology of Non-fentanyl Derived New Synthetic Opioids. Front Pharmacol. 2018;9.

3 Wang S. Historical Review: Opiate Addiction and Opioid Receptors. Cell transplant. 2019;28(3):233-38.

4 Frisoni P, Bacchio E, Bilel S, Talarico A, Gaudio RM, Barbieri M, et al. Novel Synthetic Opioids: The Pathologist's Point of View. Brain Sci. 2018;8(9).

5 Jannetto PJ, Helander A, Garg U, Janis GC, Goldberger B, Ketha H. The Fentanyl Epidemic and Evolution of Fentanyl Analogs in the United States and the European Union. Clin Chem. 2019;65(2):242-53.

6 Ventura L, Carvalho F, Dinis-Oliveira RJ. Opioids in the Frame of New Psychoactive Substances Network: A Complex Pharmacological and Toxicological Issue. Curr Mol Pharmacol. 2018;11(2):97-108.

7 Kieffer BL. Opioids: first lessons from knockout mice. Trends Pharmacol Sci. 1999;20(1):19-26.

8 Matthes HWD, Maldonado R, Simonin F, Valverde O, Slowe S, Kitchen I, et al. Loss of morphine-induced analgesia, reward effect and withdrawal symptoms in mice lacking the μ-opioid-receptor gene. Nature. 1996;383(6603):819-23.

9 Williams JT, Ingram SL, Henderson G, Chavkin C, von Zastrow M, Schulz S, et al. Regulation of mu-Opioid Receptors: Desensitization, Phosphorylation, Internalization, and Tolerance. Pharmacol Rev. 2013;65(1):223-54.

10 EMCDDA. EMCDDA, European Drug Report: Trends and Developments. 2019.

11 Prekupec MP, Mansky PA, Baumann MH. Misuse of Novel Synthetic Opioids: A Deadly New Trend. J Addict Med. 2017;11(4):256-65.

12 Kahsai AW, Xiao KH, Rajagopal S, Ahn S, Shukla AK, Sun JP, et al. Multiple ligand-specific conformations of the beta(2)-adrenergic receptor. Nat Chem Biol. 2011;7(10):692-700.

13 Liu JJ, Horst R, Katritch V, Stevens RC, Wuthrich K. Biased Signaling Pathways in beta(2)-Adrenergic Receptor Characterized by F-19-NMR. Science. 2012;335(6072):1106-10.

14 Kenakin T, Miller LJ. Seven Transmembrane Receptors as Shapeshifting Proteins: The Impact of Allosteric Modulation and Functional Selectivity on New Drug Discovery. Pharmacol Rev. 2010;62(2):265-304.

15 Wei HJ, Ahn S, Shenoy SK, Karnik SS, Hunyady L, Luttrell LM, et al. Independent beta-arrestin 2 and G protein-mediated pathways for angiotensin II activation of extracellular signal-regulated kinases 1 and 2. Proc Natl Acad Sci U.S.A. 2003;100(19):10782-87.

16 Siuda ER, Carr R, Rominger DH, Violin JD. Biased mu-opioid receptor ligands: a promising new generation of pain therapeutics. Curr Opin Pharmacol. 2017;32:77-84.

17 Raehal KM. Morphine Side Effects in -Arrestin 2 Knockout Mice. J Pharmacol Exp Ther. 2005;314(3):1195-201.

18 Violin JD, Lefkowitz RJ. β-Arrestin-biased ligands at seven-transmembrane receptors. Trends Pharmacol Sci. 2007;28(8):416-22.

19 Chen X-T, Pitis P, Liu G, Yuan C, Gotchev D, Cowan CL, et al. Structure–Activity Relationships and Discovery of a G Protein Biased μ Opioid Receptor Ligand, [(3-Methoxythiophen-2-yl)methyl]({2-[(9R)-9-(pyridin-2-yl)-6-oxaspiro-[4.5]decan-9-

yl]ethyl})amine (TRV130), for the Treatment of Acute Severe Pain. J Med Chem. 2013;56(20):8019-31.

20 Soergel DG, Subach RA, Burnham N, Lark MW, James IE, Sadler BM, et al. Biased agonism of the μ-opioid receptor by TRV130 increases analgesia and reduces on-target adverse effects versus morphine: A randomized, double-blind, placebo-controlled, crossover study in healthy volunteers. Pain. 2014;155(9):1829-35.

21 Hertz S. FDA Briefing Document. Anesthetic and Analgesic Drug Products Advisory Committee (AADPAC). 2018.

22 Vuckovic S, Prostran M, Ivanovic M, Dosen-Micovic L, Todorovic Z, Nesic Z, et al. Fentanyl Analogs: Structure-Activity-Relationship Study. Curr Med Chem. 2009;16(19):2468-74.

23 Dosen-Micovic L, Ivanovic M, Micovic V. Steric interactions and the activity of fentanyl analogs at the mu-opioid receptor. Bioorgan Med Chem. 2006;14(9):2887-95.

24 Mićović IV, Ivanović MD, Vuckovic SM, Prostran MŠ, Došen-Mićović L, Kiricojević VD. The Synthesis and preliminary pharmacological evaluation of 4-Methyl fentanyl. Bioorg Med Chem Lett. 2000;10(17):2011-14.

25 Vuckovic S, Prostran M, Ivanovic M, Ristovic Z, Stojanovic R. Antinociceptive Activity of the Novel Fentanyl Analogue iso-Carfentanil in Rats. Jpn J Pharmacol. 2000;84(2):188-95.

26 Wilde M, Pichini S, Pacifici R, Tagliabracci A, Busardò FP, Auwärter V, et al. Metabolic Pathways and Potencies of New Fentanyl Analogs. Front Pharmacol. 2019;10.

27 Ehrlich AT, Semache M, Gross F, Da Fonte DF, Runtz L, Colley C, et al. Biased Signaling of the Mu Opioid Receptor Revealed in Native Neurons. Iscience. 2019;14:47-+.

28 Schmid CL, Kennedy NM, Ross NC, Lovell KM, Yue ZZ, Morgenweck J, et al. Bias Factor and Therapeutic Window Correlate to Predict Safer Opioid Analgesics. Cell. 2017;171(5):1165-+.

29 Nehme R, Carpenter B, Singhal A, Strege A, Edwards PC, White CF, et al. Mini-G proteins: Novel tools for studying GPCRs in their active conformation. Plos One. 2017;12(4).

30 Wan Q, Okashah N, Inoue A, Nehmé R, Carpenter B, Tate CG, et al. Mini G protein probes for active G protein–coupled receptors (GPCRs) in live cells. J Biol Chem. 2018;293(19):7466-73.

31 Dixon AS, Schwinn MK, Hall MP, Zimmerman K, Otto P, Lubben TH, et al. NanoLuc Complementation Reporter Optimized for Accurate Measurement of Protein Interactions in Cells. Acs Chem Biol. 2015;11(2):400-08.

32 Cannaert A, Vasudevan L, Friscia M, Mohr ALA, Wille SMR, Stove CP. Activity-Based Concept to Screen Biological Matrices for Opiates and (Synthetic) Opioids. Clin Chem. 2018;64(8):1221-29.

33 Wouters E, Walraed J, Robertson MJ, Meyrath M, Szpakowska M, Chevigné A, et al. Assessment of Biased Agonism among Distinct Synthetic Cannabinoid Receptor Agonist Scaffolds. ACS Pharmacol. Transl. Sci. 2019.

34 Cannaert A, Storme J, Franz F, Auwärter V, Stove CP. Detection and Activity Profiling of Synthetic Cannabinoids and Their Metabolites with a Newly Developed Bioassay. Anal Chem. 2016;88(23):11476-85.

35 Cannaert A, Franz F, Auwärter V, Stove CP. Activity-Based Detection of Consumption of Synthetic Cannabinoids in Authentic Urine Samples Using a Stable Cannabinoid Reporter System. Anal Chem. 2017;89(17):9527-36.

36 Zhang J, Ferguson SSG, Barak LS, Bodduluri SR, Laporte SA, Law PY, et al. Role for G protein-coupled receptor kinase in agonist-specific regulation of -opioid receptor responsiveness. Proc Natl Acad Sci U.S.A. 1998;95(12):7157-62.

37 Blanckaert P, Cannaert A, Van Uytfanghe K, Hulpia F, Deconinck E, Van Calenbergh S, et al. Report on a novel emerging class of highly potent benzimidazole NPS opioids: Chemical and in vitro functional characterization of isotonitazene. Drug Test Anal. 2020. In Press. https://doi.org/10.1002/dta.2738

38 Gundry J, Glenn R, Alagesan P, Rajagopal S. A Practical Guide to Approaching Biased Agonism at G Protein Coupled Receptors. Front Neurosci-Switz. 2017;11.

39 Winpenny D, Clark M, Cawkill D. Biased ligand quantification in drug discovery: from theory to high throughput screening to identify new biased μ opioid receptor agonists. Brit J Pharmacol. 2016;173(8):1393-403.

40 Pasternak GW, Pan Y-X, Sibley DR. Mu Opioids and Their Receptors: Evolution of a Concept. Pharmacol Rev. 2013;65(4):1257-317.

41 Al-Hasani R, Bruchas MR. Molecular Mechanisms of Opioid Receptor-dependent Signaling and Behavior. Anesthesiology. 2011;115:1363-81.

42 Laycock H, Bantel C. Opioid mechanisms and opioid drugs. Anaesth Intensive Care. 2019;20(8):450-55.

43 Berlin S, Keren-Raifman T, Castel R, Rubinstein M, Dessauer CW, Ivanina T, et al. Gαiand Gβγ Jointly Regulate the Conformations of a Gβγ Effector, the Neuronal G Protein-activated K+Channel (GIRK). J Biol Chem. 2010;285(9):6179-85.

44 Kahanovitch U, Tsemakhovich V, Berlin S, Rubinstein M, Styr B, Castel R, et al. Recruitment of Gβγ controls the basal activity of G-protein coupled inwardly rectifying potassium (GIRK) channels: crucial role of distal C terminus of GIRK1. J Physiol. 2014;592(24):5373-90.

45 Lei Q JM, Talley EM, Garrison JC, Bayliss DA. Molecular Mechanisms Mediating Inhibition of G Protein-coupled Inwardly-rectifying K+ Channels. Mol Cells. 2003;15:1-9.

46 DeFea K. β-arrestins and heterotrimeric G-proteins: collaborators and competitors in signal transduction. Brit J Pharmacol. 2009;153(S1):S298-S309.

47 DeWire SM, Ahn S, Lefkowitz RJ, Shenoy SK. β-Arrestins and Cell Signaling. Annu Rev Physiol. 2007;69(1):483-510.

48 McPherson J, Rivero G, Baptist M, Llorente J, Al-Sabah S, Krasel C, et al. mu-Opioid Receptors: Correlation of Agonist Efficacy for Signalling with Ability to Activate Internalization. Mol Pharmacol. 2010;78(4):756-66.

49 Rajagopal S, Rajagopal K, Lefkowitz RJ. Teaching old receptors new tricks: biasing seven-transmembrane receptors. Nat Rev Drug Discov. 2010;9(5):373-86.

50 Kruegel AC, Uprety R, Grinnell SG, Langreck C, Pekarskaya EA, Le Rouzic V, et al. 7-Hydroxymitragynine Is an Active Metabolite of Mitragynine and a Key Mediator of Its Analgesic Effects. ACS Cent. Sci. 2019;5(6):992-1001.

51 Manglik A, Lin H, Aryal DK, McCorvy JD, Dengler D, Corder G, et al. Structure-based discovery of opioid analgesics with reduced side effects. Nature. 2016;537(7619):185-90.

52 Grim TW, Acevedo-Canabal A, Bohn LM. Toward Directing Opioid Receptor Signaling to Refine Opioid Therapeutics. Biol Psychiat. 2020;87(1):15-21.

53 Kliewer A, Gillis A, Hill R, Schmidel F, Bailey C, Kelly E, et al. Morphine-induced respiratory depression is independent of β-arrestin2 signalling. Br J Pharmacol. 2020. In Press. https://doi.org/10.1111/bph.15004

54 Wouters E, Walraed J, Banister SD, Stove CP. Insights into biased signaling at cannabinoid receptors: synthetic cannabinoid receptor agonists. Biochem Pharmacol. 2019;169.

55 Smith JS, Lefkowitz RJ, Rajagopal S. Biased signalling: from simple switches to allosteric microprocessors. Nat Rev Drug Discov. 2018;17(4):243-60.

56 Rajagopal S, Ahn S, Rominger DH, Gowen-MacDonald W, Lam CM, DeWire SM, et al. Quantifying Ligand Bias at Seven-Transmembrane Receptors. Mol Pharmacol. 2011;80(3):367-77.

57 Klein Herenbrink C, Sykes DA, Donthamsetti P, Canals M, Coudrat T, Shonberg J, et al. The role of kinetic context in apparent biased agonism at GPCRs. Nat Commun. 2016;7(1).

58 DeWire SM, Yamashita DS, Rominger DH, Liu G, Cowan CL, Graczyk TM, et al. A G Protein-Biased Ligand at the μ-Opioid Receptor Is Potently Analgesic with Reduced Gastrointestinal and Respiratory Dysfunction Compared with Morphine. J Pharmacol Exp Ther. 2013;344(3):708-17.

Figure Legends

Figure 1: Overview of the 22 evaluated compounds (21 synthetic opioids and TRV130), with structural classification of the fentanyl analogues based on the nature of the R_1 group (**Panel A**). **Panel B**: R_1 group is aliphatic; **Panel C**: R_1 group is ether or aromatic; **Panel D**: Other; **Panel E**: Non-fentanyl synthetic opioids; **Panel F**: TRV130. All the fentanyl analogues carry an 'H' atom at the R_2 and R_3 position, unless:

(a): the R_2 is a methoxy group in 4-methoxybutyrylfentanyl **(4)** and a fluorine atom in 4-fluoroisobutyrylfentanyl **(5)**

(b): R_3 is a fluorine atom in ocfentanil **(14)**

Figure 2: Set-up for the determination of the optimal combination for the MOR-mini-Gi reporter system: 4 configurations were used for transiently transfecting HEK293T cells: MOR-LgBiT + mini-Gi-SmBiT / MOR-LgBiT+ SmBiT-mini-Gi / MOR-SmBiT + mini-Gi-LgBiT / MOR-SmBiT+ LgBiT-mini-Gi. Upon stimulation with 10 µM HM (0), the luminescence was measured up to 120 min. Data depicts average fold change ± SD (n=6) of the stimulated well (filled bars) over the unstimulated well (solvent control) (open bars). The frame indicates the combination that was chosen for further experiments. ** $p \leq 0.001$ (two-tailed t-test).

Figure 3: Stability of the stable cell lines over time: The plots depict MOR: mini-Gi **(A)** and MOR: βarr2: GRK2 **(B)**. The percentage of double positive expressing cells in the case of MOR: mini-Gi and percentage of triple positive in the case of MOR: βarr2: GRK2 (% Q2) are mentioned in the table. EGFP is a measure of MOR, APC for mini-Gi / βarr2, and BV for GRK2. (P: passage)

Figure 4: Sigmoidal dose-response curves generated for 18 fentanyl analogues, 3 other opioids and TRV130, in addition to the reference compound HM **(0)**, using the developed stable NanoBiT®

MOR reporter assays for coupling of mini-Gi (**black curve**) and recruitment of βarr2 (**red curve**). The curves are represented as AUC (± SEM) for three independent experiments, normalized to the reference agonist HM **(0)**. Please note the difference in the scales of the Y-axis.

Figure 5: Comparison of efficacies (E_{max}) (A) and potencies (pEC_{50}) (B) for 21 synthetic opioids and TRV130 **(22)**, relative to HM **(0)** (arbitrarily set to 100%), tested for their capacity to recruit mini-Gi or βarr2 to MOR using NanoBiT® in stable cell lines.

Figure 6: Quantitative pathway bias plot for all the fentanyl, non-fentanyl opioids and TRV130 **(22)**: Values are represented as Δlog (E_{max}/EC_{50}) mini-Gi - Δlog (E_{max}/EC_{50}) βarr2 ± SEM (a measure of bias). None of the compounds showed a significant bias, when compared to the reference HM **(0)**.

Table 1: List of primers used in the study: Primers used for cloning of MOR-LgBiT and GRK2 in pDONR™. Forward (F) and Reverse (R) primers (5' →3') with kozak sequence (underlined) and recombination sequence (in grey) for ***MOR-LgBiT (A) and GRK2 (B)*** (coding sequences in bold, italics), For GRK2, a two-step nested-PCR amplification was followed, first with primer set F1 and R1 and, using the amplified product from reaction 1, a second PCR with primer set F2 and R2. The annealing temperature used for all the PCRs was 72°C.

Table 2: Efficacy (E_{max}), potency (pEC_{50}) and bias factor of 18 fentanyl analogues, 3 non-fentanyl synthetic opioids, TRV130 **(22)** and the reference compound, HM **(0),** obtained from both reporter assays (mini-Gi and β-arrestin2), ordered according to the structural classification depicted in **Figure 1.**

Figure 1

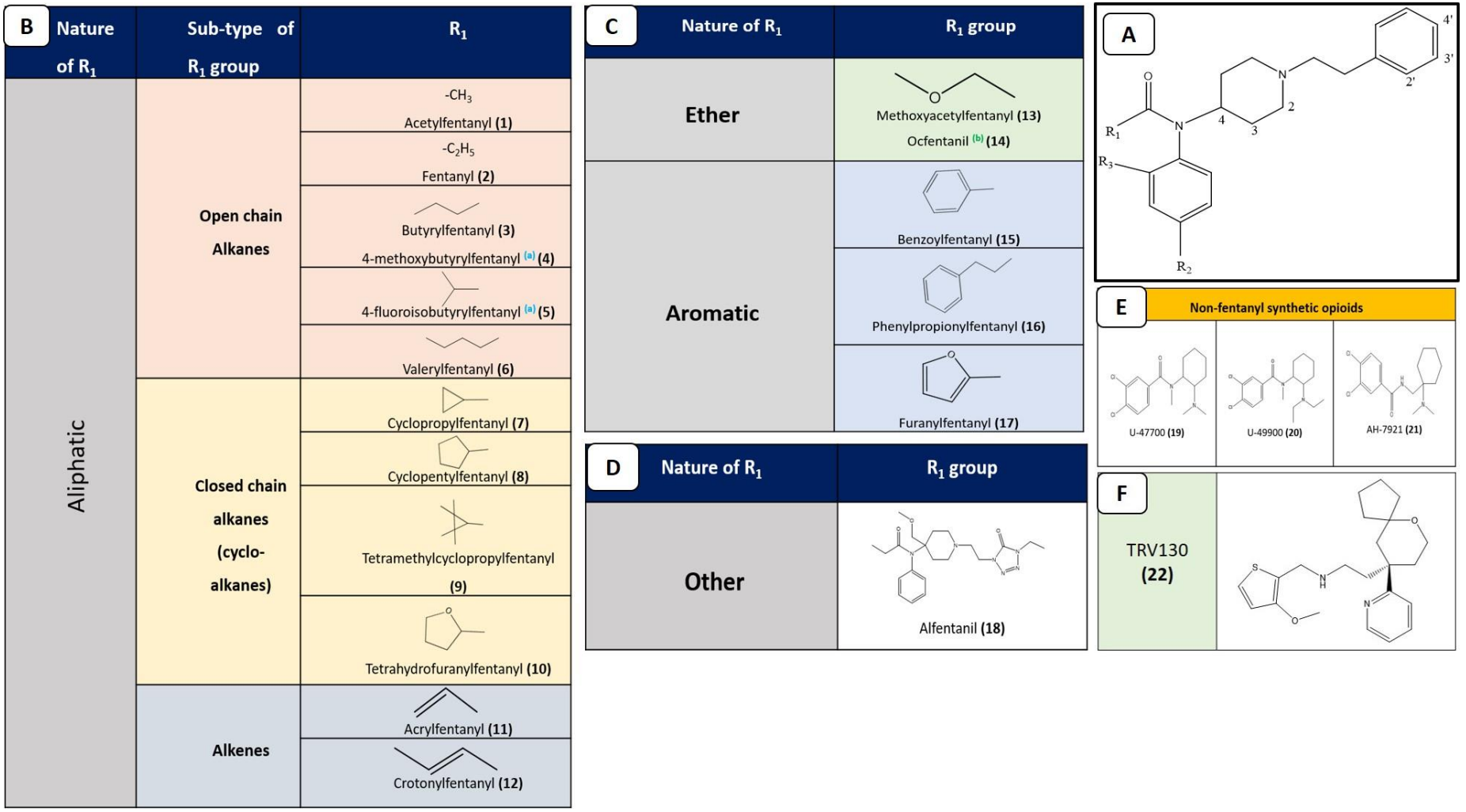
B
Nature of R_1
Sub-type of R_1 group
R_1
Aliphatic
Open chain Alkanes
$-CH_3$
Acetylfentanyl (1)
$-C_2H_5$
Fentanyl (2)
Butyrylfentanyl (3)
4-methoxybutyrylfentanyl [a] (4)
4-fluoroisobutyrylfentanyl [a] (5)
Valerylfentanyl (6)
Closed chain alkanes (cyclo-alkanes)
Cyclopropylfentanyl (7)
Cyclopentylfentanyl (8)
Tetramethylcyclopropylfentanyl (9)
Tetrahydrofuranylfentanyl (10)
Alkenes
Acrylfentanyl (11)
Crotonylfentanyl (12)
C
Nature of R_1
R_1 group
Ether
Methoxyacetylfentanyl (13)
Ocfentanil [b] (14)
Aromatic
Benzoylfentanyl (15)
Phenylpropionylfentanyl (16)
Furanylfentanyl (17)
D
Nature of R_1
R_1 group
Other
Alfentanil (18)
A
E
Non-fentanyl synthetic opioids
U-47700 (19)
U-49900 (20)
AH-7921 (21)
F
TRV130 (22)

Figure 2

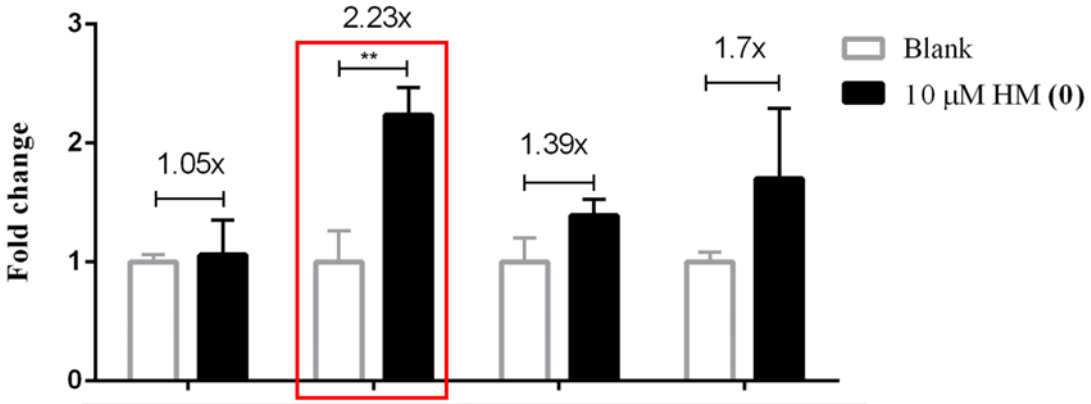

MOR-LgBiT	MOR-LgBiT	MOR-SmBiT	MOR-SmBiT
mini-Gi-SmBiT	SmBiT-mini-Gi	mini-Gi-LgBiT	LgBiT-mini-Gi

Figure 3

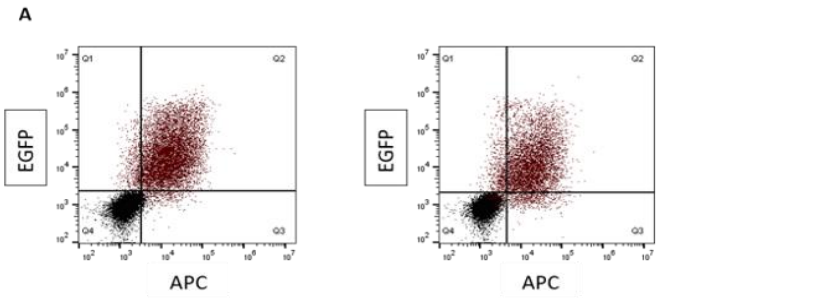

P=1	Sample name	% Q2
	MOR: mini-Gi	89
	HEK293T (negative control)	0.06

P=13	Sample name	% Q2
	MOR: mini-Gi	81
	HEK293T (negative control)	0

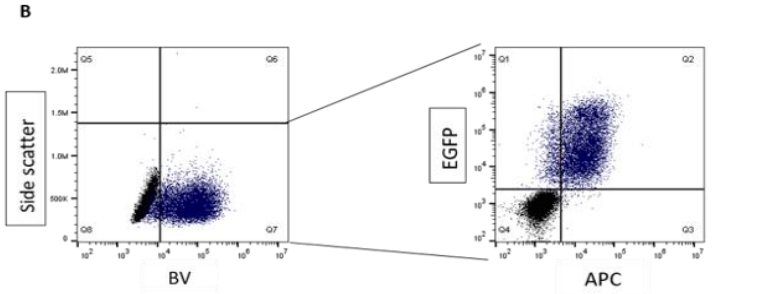

P=1	Sample name	% Q7
	GRK2	93
	HEK293T (negative control)	0.04

P=1	Sample name	% Q2
	MOR: βarr2: GRK2	89
	HEK293T (negative control)	0

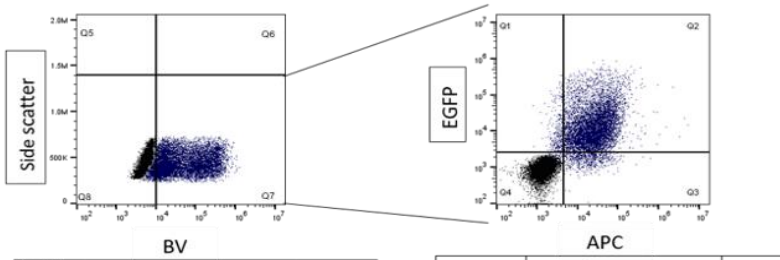

P=13	Sample name	% Q7
	GRK2	92
	HEK293T (negative control)	0.08

P=13	Sample name	% Q2
	MOR: βarr2 : GRK2	87
	HEK293T (negative control)	0

Figure 4

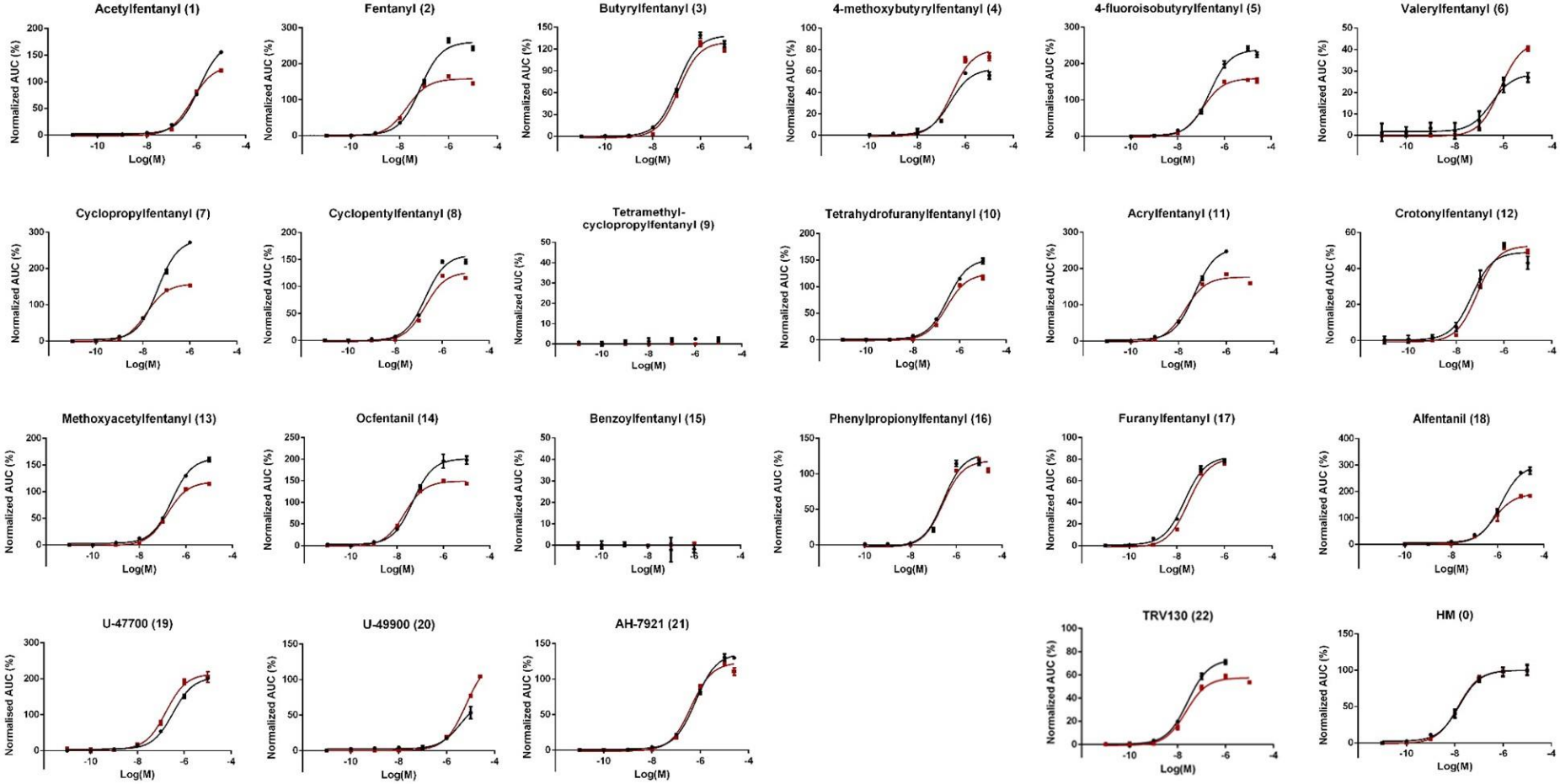
Acetylfentanyl (1)
Fentanyl (2)
Butyrylfentanyl (3)
4-methoxybutyrylfentanyl (4)
4-fluoroisobutyrylfentanyl (5)
Valerylfentanyl (6)
Cyclopropylfentanyl (7)
Cyclopentylfentanyl (8)
Tetramethyl-cyclopropylfentanyl (9)
Tetrahydrofuranylfentanyl (10)
Acrylfentanyl (11)
Crotonylfentanyl (12)
Methoxyacetylfentanyl (13)
Ocfentanil (14)
Benzoylfentanyl (15)
Phenylpropionylfentanyl (16)
Furanylfentanyl (17)
Alfentanil (18)
U-47700 (19)
U-49900 (20)
AH-7921 (21)
TRV130 (22)
HM (0)
Normalized AUC (%)
Log(M)

Figure 5

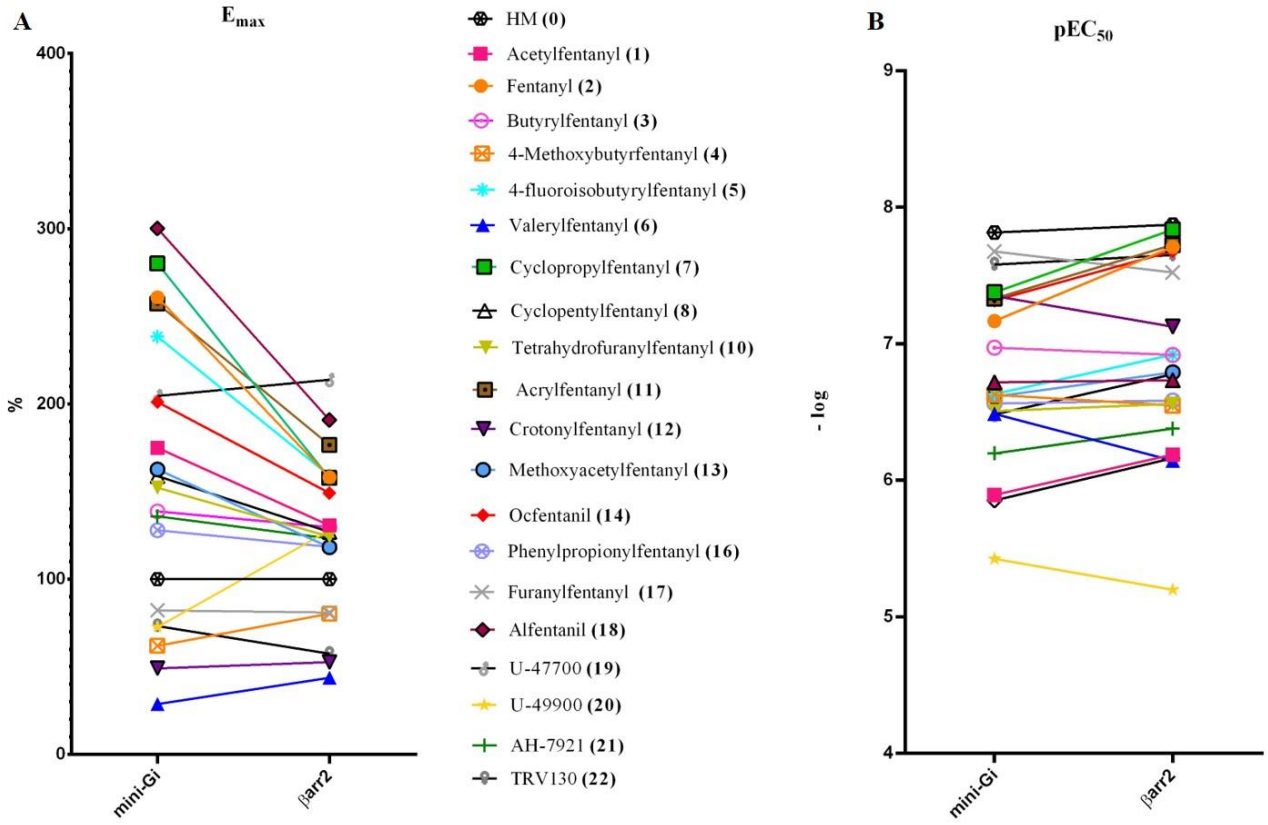
A
Emax
400
300
200
100
0
%
mini-Gi
βarr2
HM (0)
Acetylfentanyl (1)
Fentanyl (2)
Butyrylfentanyl (3)
4-Methoxybutyrfentanyl (4)
4-fluoroisobutyrylfentanyl (5)
Valerylfentanyl (6)
Cyclopropylfentanyl (7)
Cyclopentylfentanyl (8)
Tetrahydrofuranylfentanyl (10)
Acrylfentanyl (11)
Crotonylfentanyl (12)
Methoxyacetylfentanyl (13)
Ocfentanil (14)
Phenylpropionylfentanyl (16)
Furanylfentanyl (17)
Alfentanil (18)
U-47700 (19)
U-49900 (20)
AH-7921 (21)
TRV130 (22)
B
pEC50
9
8
7
6
5
4
- log
mini-Gi
βarr2

Figure 6

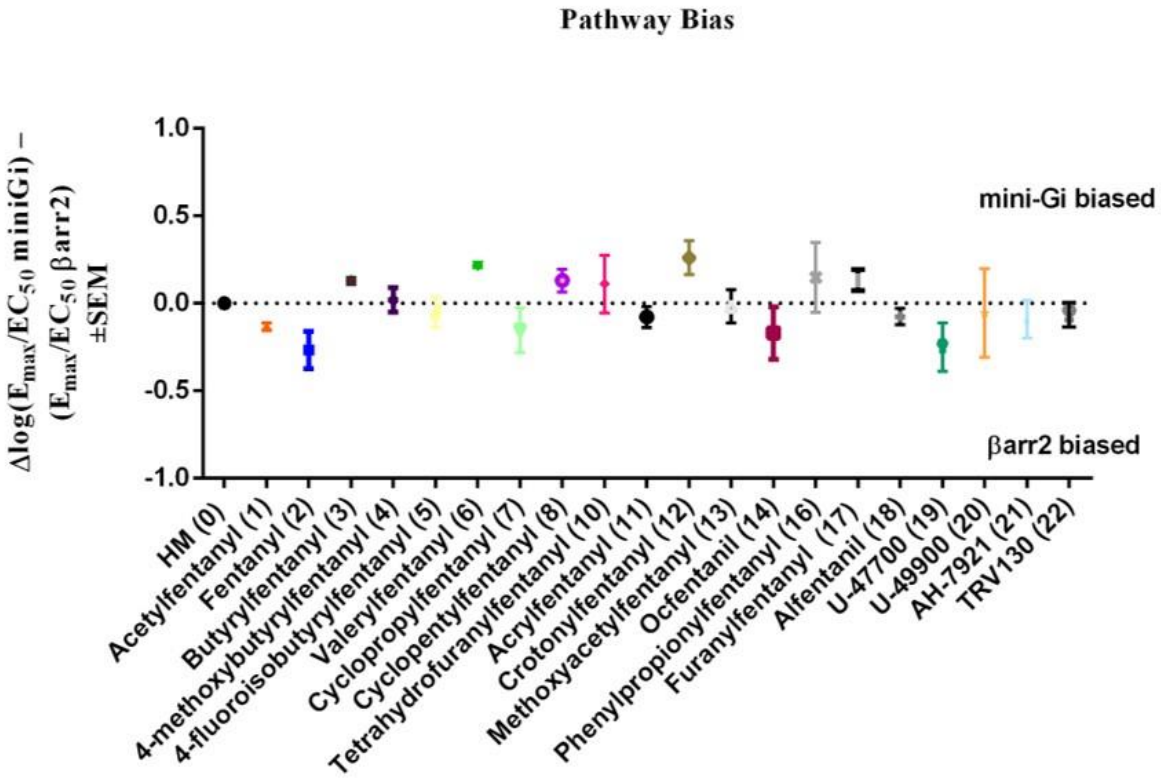
Pathway Bias
Δlog(Emax/EC50 miniGi) – (Emax/EC50 βarr2) ±SEM
1.0
0.5
0.0
-0.5
-1.0
mini-Gi biased
βarr2 biased
HM (0)
Acetylfentanyl (1)
Fentanyl (2)
Butyrylfentanyl (3)
4-methoxybutyrylfentanyl (4)
4-fluoroisobutyrylfentanyl (5)
Valerylfentanyl (6)
Cyclopropylfentanyl (7)
Cyclopentylfentanyl (8)
Tetrahydrofuranylfentanyl (10)
Acrylfentanyl (11)
Crotonylfentanyl (12)
Methoxyacetylfentanyl (13)
Ocfentanil (14)
Phenylpropionylfentanyl (16)
Furanylfentanyl (17)
Alfentanil (18)
U-47700 (19)
U-49900 (20)
AH-7921 (21)
TRV130 (22)

Table 1

A

Insert	Primers	
MOR-LgBiT	F	GGGGACAAGTTTGTACAAAAAAGCAGGCTTCACC***ATGGACAGCAGC***
	R	GGGGACCACTTTGTACAAGAAAGCTGGGTA***TTAGCTGTTGATGGTTACTCGG***

B

Insert	Primers	
GRK2	F2	GGGGACAAGTTTGTACAAAAAAGCAGGCTTCACC
	F1	AGGCTTCACC ***ATGGCGGACCTGGAGGC***
	R1	GAAAGCTGGGTA***TCAGAGGCCGTTGGCACTGCC***
	R2	GGGGACCACTTTGTACAAGAAAGCTGGG

Table 2

Compound	Mini-Gi assay		β-arrestin2 assay		Bias factor
	E_{max} (%) ± SEM	$LogEC_{50}$ ± SEM	E_{max} (%) ± SEM	$LogEC_{50}$ ± SEM	
Hydromorphone (0)	**100 ± 2.77**	**- 7.816 ± 0.09**	**100 ± 2.16**	**-7.873 ± 0.06**	**0**
Acetylfentanyl (1)	175± 3.32	- 5.892 ± 0.03	131 ± 2.43	- 6.188 ± 0.03	-0.13
Fentanyl (2)	261 ± 6.00	- 7.167 ± 0.06	158 ± 2.95	-7.709 ± 0.06	-0.27
Butyrylfentanyl (3)	139 ± 4.04	- 6.971 ± 0.07	130 ± 3.55	- 6.919 ± 0.06	0.13
4-Methoxybutyrylfentanyl (4)	61.9 ± 3.21	-6.626 ± 0.12	80.3 ± 3.55	- 6.548 ± 0.10	0.02
4-Fluoro-isobutyrylfentanyl (5)	238 ± 4.61	- 6.631 ± 0.06	159 ± 2.27	- 6.920 ± 0.04	-0.05
Valerylfentanyl (6)	28.6 ± 3.21	- 6.487 ± 0.27	43.7 ± 0.90	- 6.144 ± 0.04	0.21
Cyclopropylfentanyl (7)	280 ± 4.56	- 7.376 ± 0.04	158 ± 1.48	- 7.837 ± 0.02	-0.15
Cyclopentylfentanyl (8)	159 ± 4.71	- 6.717 ± 0.07	127 ± 3.82	- 6.733 ± 0.07	0.13
Tetramethylcyclopropylfentanyl (9)	ND	ND	ND	ND	ND
Tetrahydrofuranylfentanyl (10)	152 ± 2.50	- 6.507 ± 0.04	124 ± 2.59	- 6.560 ± 0.05	0.11
Acrylfentanyl (11)	258 ± 4.15	- 7.332 ± 0.03	177 ± 3.84	- 7.725 ± 0.06	-0.08
Crotonylfentanyl (12)	49.0 ± 2.44	- 7.351 ± 0.14	52.6 ± 1.10	- 7.125 ± 0.05	0.26
Methoxyacetylfentanyl (13)	163 ± 2.29	- 6.612 ± 0.03	118 ± 1.31	- 6.791 ± 0.03	-0.02
Ocfentanil (14)	201 ± 5.18	- 7.318 ± 0.07	149 ± 1.70	- 7.679 ± 0.03	-0.17
Benzoylfentanyl (15)	ND	ND	ND	ND	ND
Phenylpropionylfentanyl (16)	128 ± 5.98	- 6.562 ± 0.11	118 ± 3.69	- 6.584 ± 0.09	0.15
Furanylfentanyl (17)	82.2 ± 1.74	- 7.676 ± 0.05	81.0 ± 1.98	- 7.522 ± 0.06	0.13
Alfentanil (18)	300 ± 7.12	- 5.852 ± 0.06	191 ± 6.72	- 6.162 ± 0.09	-0.08
U-47700 (19)	205 ± 3.75	- 6.482 ± 0.04	214 ± 6.35	- 6.776 ± 0.08	-0.25
U-49900 (20)	72.6 ± 10.85	- 5.424 ± 0.2	128 ± 3.19	-5.197 ± 0.03	-0.06
AH-7921 (21)	136 ± 2.41	- 6.196 ± 0.04	123 ± 2.35	- 6.379 ± 0.04	-0.09
TRV130 (22)	73.2 ± 1.5	-7.580 ± 0.05	57.4 ± 1.16	-7.650 ± 0.07	-0.07

E_{max} represented here is relative to that of the reference agonist HM **(0)**, which is arbitrarily set to 100%. **ND:** not determined